Heliyon 10 (2024) e26054

Contents lists available at ScienceDirect

Heliyon

journal homepage: www.cell.com/heliyon

Research article

Wave absorbing properties of Ni Nanoparticle/CNT composite film fabricated by AAO/CNTs electrode

Zhenxing Song [a,*,1], Yue Yang [a], Panchao Hou [a], Xiaorui Zhang [a], Shan Liang [a], Jun Chen [b]

[a] School of Science, Tianjin University of Science and Technology, Tianjin 300450, China
[b] Hunan Kejing New Energy Technology Co., Ltd., China

ARTICLE INFO

Keywords:
Microwave absorbing
Electrodeposition
AAO/CNTs electrode
Ni nano particles
Carbon nanotubes

ABSTRACT

An effective wave absorbing Nano-Ni/carbon nanotubes (CNTs) composite film was developed by electrodeposition using an anodic aluminum oxide (AAO)/CNTs electrode. Scanning electron microscopy images confirmed the uniform dispersion of Ni nano-particles within the CNTs, and the particle diameter increasing from 20 nm to 100 nm as the deposition time increased. XRD test results revealed that the crystal phase of the Ni nano-particles remained unchanged during different deposition time, exhibiting a Face Center Cubic (fcc) structure. The microwave electromagnetic properties of the film were evaluated using a vector network analyzer, and the return loss curve demonstrated that the Ni nano-particles/CNTs composite exhibited exceptional wave absorption capabilities. The composite film showed an effective absorption width of 13 GHz (4–17 GHz) and achieved a minimum reflection loss (RL) of −17 dB at 14 GHz.

1. Introduction

Microwave absorbing materials (WAMs) have gained significant global attention due to the growing issue of increasing electromagnetic interference [1–6]. Nanostructured materials, among various WAMs, have emerged as promising candidates for efficient electromagnetic wave absorption due to their unique properties [7–9]. Sun et al. [10] synthesized $NiCo_2$-0.5xCr_2O_3@C nanocomposites an impressive reflection loss (RL) of −52.71 dB at 1.6 mm and an effective absorption bandwidth (EAB) of 5.28 GHz at 1.89 mm. Wang et al. prepared [11] FeO_X/CSBC nanocomposites with a minimum RL peak of −29.5 dB and an EAB of 6.4 GHz at an absorber thickness of 2.7 mm. Hassan et al. [12] achieved UCESM@CF composite with a RL peak of −39.03 dB at 10.44 GHz, using in-situ grew CF nanoparticles.

Nickel (Ni) nanoparticles have been extensively researched as excellent electromagnetic absorbers [13,14]. The Ni@Co/C@PPy composite prepared by Bi et al. [15] showed excellent electromagnetic wave absorption performance when the corresponding thickness was 2.0 mm. The RL value was −48.76 dB and the effective absorption bandwidth was 5.10 GHz. Liu et al. [16] utilized a simple wet chemical method to fabricate a three-dimensional nickel chain link mesh with a thickness of 1.8 mm at 8.8 GHz and 373 K achieving the maximum absorption value was −50 dB. However, particle aggregation frequently hinders their absorption performance resulting in decreased effectiveness [17,18].

* Corresponding author.
E-mail address: szx@tust.edu.cn (Z. Song).
[1] Present address: Tianjin University of Science and Technology, Tianjin 300450, China.

https://doi.org/10.1016/j.heliyon.2024.e26054
Received 25 November 2023; Received in revised form 7 February 2024; Accepted 7 February 2024
Available online 17 February 2024

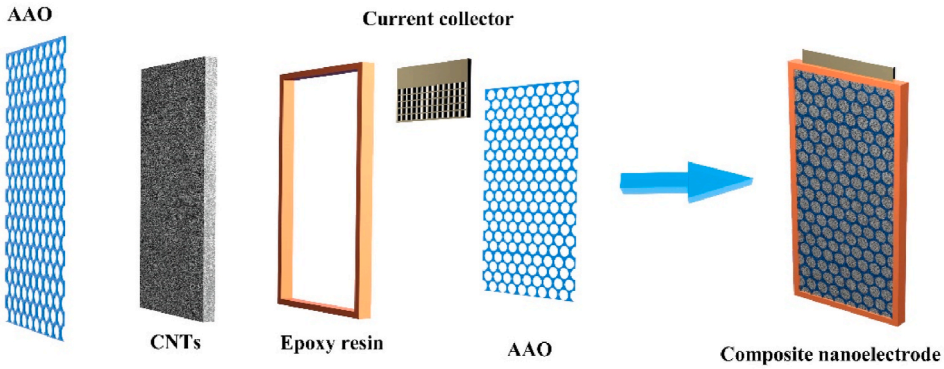

Fig. 1. Schematic illustration of AAO/CNTs electrode.

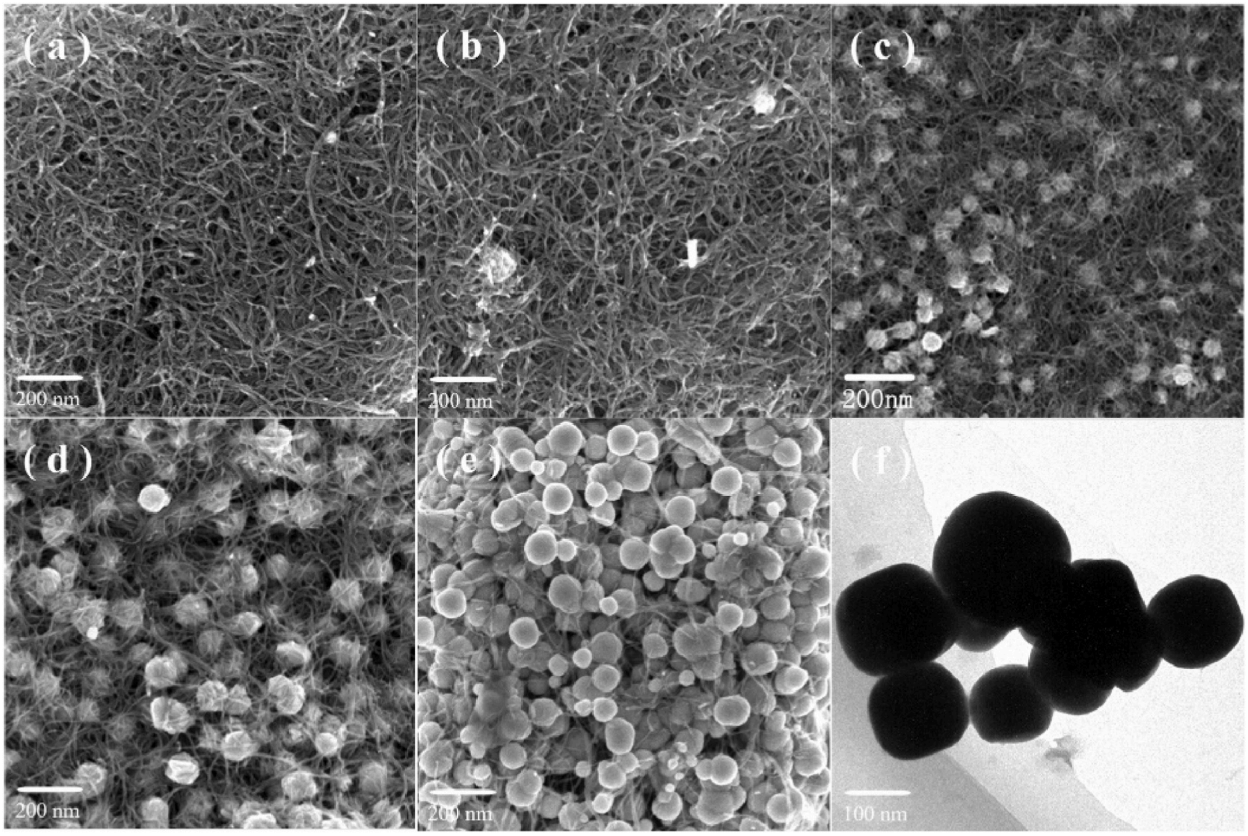

Fig. 2. SEM pictures of Ni nano-particles/CNTs composite after deposition of different periods (a) 1 min, (b) 2 min, (c) 5 min, (d) 10 min, (e) 15 min; (f) TEM picture of Ni nano particles.

Nano-Ni/CNTs film was manufactured by a novel anodic aluminum oxide (AAO)/Carbon nanotubes (CNTs) electrode in this article. The inclusion of CNTs in the films prevents aggregation of nano-Ni particles. Moreover, the diameter of the particles can be precisely controlled by changing the electrodeposition time [19–21]. The wave absorption performance of the Ni nano-particles/CNTs film was confirmed using a vector network analyzer. This film offers advantages such as simplification of operation, mild reaction conditions, high purity of the obtained nanoparticles, low environmental pollution.

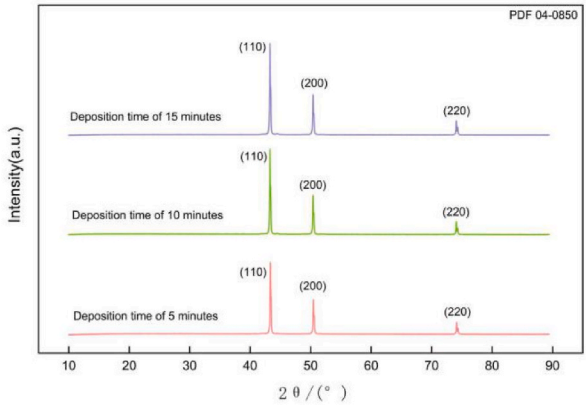

Fig. 3. XRD patterns of Ni nano-particles/CNTs composite.

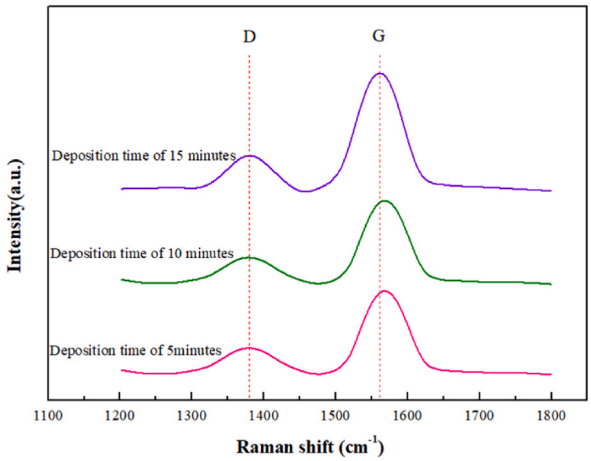

Fig. 4. Normal Raman spectra of Ni nano-particles/CNTs composite.

2. Experimental section

2.1. Material preparation

The AAO/CNTs electrode (Fig. 1) was assembled using AAO [22], CNTs, and a copper current collector. A container was utilized to encapsulate the CNTs, eliminating the need off glue and improving the conductivity, purity, surface charge distribution, and electrochemical activity of the CNTs.

The AAO/CNTs electrode was applied as the working electrode in a conventional three-electrode direct current (DC) electrodeposition system, with a saturated calomel electrode (SCE) as the reference electrode and a platinum plate measuring 1.0 cm * 1.0 cm as the counter electrode. The electrolyte consisted of 180 g/L $NiSO_4$, while of the current density was strictly controlled to be 3 mA/cm^2.

Following electrodeposition, the AAO on the electrode was dissolved in 1 M NaOH solution, thus the nano-Ni/CNTs composite was obtained. The composites were subsequently subjected to ultrasound treatment in alcohol to yield nickel nanoparticles.

2.2. Characterization

The morphology of the samples was observed by scanning electron microscopy (SEM, ZEISS, EVO18) and transmission electron microscopy (TEM, Tescan G2 F20). The X-ray diffraction (XRD, BRUKER D8 ADVANCE) method was employed to determine the crystalline structure of the samples. The Raman study of samples was performed with a HORIBA HR Evolution Raman Microscope. The magnetic properties of the samples were evaluated utilizing Vector Network Analyser Type N5242A.

3. Results and discussion

The images from Fig. 2a–e demonstrate the uniform dispersion of Ni nanoparticles in CNTs. As the deposition time increased, the

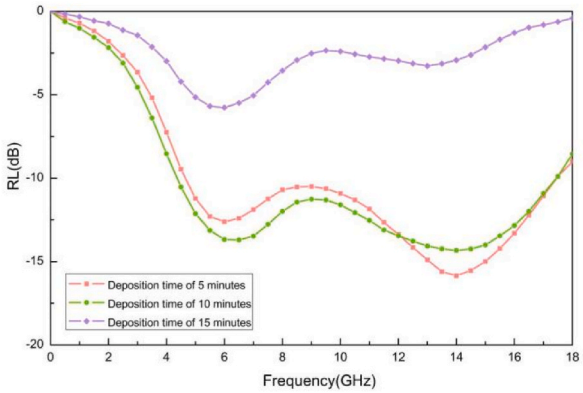

Fig. 5. RL values of Ni nano-particles/CNTs composite with different deposition time.

diameter of the nickel nanoparticles grew from 20 nm to 100 nm, and the surface of the particles became progressively smoother while the step-like grain boundaries gradually disappeared.

During the initial stage of electrodeposition (Fig. 2a), metal crystal seeds appeared at the intersections of nanotubes, where the overpotential is highest. Due to the binding and obstruction of carbon nanotubes, further electro-crystallization could only occur along the grain boundaries of these crystal seeds, thereby avoiding particle aggregation (Fig. 2a–c).

After the deposition, the AAO template was removed, and the Ni nano-particles/CNTs electrode were illustrated in Fig. 2d and e. It can be observed that the sample consisted of a large quantity of Ni nanoparticles with a diameter of 100 nm (Fig. 2f).

Fig. 3 shows the XRD patterns of Ni nanoparticles deposited for 5 min, 10 min, and 15 min, respectively. The diffraction peaks of Ni can be observed at 2θ angles of 44.98°, 52.28°, and 74.99°, corresponding to the crystal planes (110), (200), and (220), respectively. The crystal structure was determined to be a close-packed hexagonal (fcc) structure (PDF 04-0850). Increasing of particle diameter did not significantly alter the width of the diffraction peaks, whilst the intensity ratio of each crystal plane slightly changed accordingly. It suggests that changes in the diameter and number of Ni nanoparticles do not have a substantial impact on the crystal phase and grain size.

Fig. 4 presents the typical Raman spectra of Ni nanoparticles deposited for 5 min, 10 min, and 15 min. These spectra exhibit prominent peaks corresponding to the D-band and G-band. The D-band peak is attributed to disordered sp^3 carbon or defects at the crystalline edges of graphitic carbon, while the G-band peak is associated with graphitic carbon sp^2 carbon correlation [23,24]. In comparison to the Ni nanoparticles deposited for 5 min and 10 min, the Ni nanoparticles deposited for 15 min show a red shift in the G-band, indicating that most of the carbon nanotubes (CNTs) were coated by Ni.

The integrated intensity ratio of the D-band to the G-band (I_D/I_G) is commonly recognized as an indicator of the degree of graphitization [25,26]. For the Ni nanoparticles deposited for 5 min, 10 min, and 15 min, the calculated I_D/I_G values are 0.42, 0.40, and 0.33, respectively. The I_D/I_G values of the samples deposited for 5 min and 10 min are higher than those deposited for 15 min, which indicates that the carbon in the samples contains a significant number of structural defects and exhibits a lower degree of graphitization. The lower degree of graphitization facilitates impedance matching, reduces surface reflection, and allows for increased penetration of electromagnetic waves into the material [2,27].

In order to investigate the electromagnetic wave absorption properties of Ni nano-particles/CNTs composites, return loss (RL) of different deposition times was calculated [1,9–11], as shown in Fig. 5. The absorption values of the lower frequency peak (LP) and higher frequency peak (HP) were measured for varying deposition times. When the deposition time was 5 min, the absorption value of LP was approximately −12.5 dB and the value of HP was around −17 dB, while the bandwidth is about 12.5 GH_Z. As the deposition time increased to 10 min, the absorption value of LP reached −13.5 dB while the value of HP shifted to −14 dB and the bandwidth was slightly expanded to 13 GHz. However, when the deposition time was 15 min, the absorption value failed to meet the required demand ($RL < -10$ dB). This result may be attributed to the fact that most of the CNTs were coated by Ni and many Ni nanoparticles aggregated leading to the disappearance of the Ni nanostructure. Based on these experiments, it can be concluded that Ni nano-particles/CNTs composites with deposition times of 5 and 10 min exhibited better electromagnetic wave absorption performance.

4. Conclusion

Utilizing an AAO/CNTs electrode, nickel nanoparticles were successfully synthesized with a close-packed hexagonal (fcc) structure. The crystal phase and grain size remained unchanged despite alterations in the diameter and quantity of the particles. This method proved to be a successful fabrication technique for metal nanoparticles. Furthermore, the Ni nanoparticle/CNT composite demonstrated exceptional wave absorption with a minimum absorption value of −17 dB and an absorption bandwidth of 13 GHz.

CRediT authorship contribution statement

Zhenxing Song: Writing – review & editing, Conceptualization. **Yang Yue:** Writing – original draft, Formal analysis, Data curation. **Panchao Hou:** Writing – review & editing. **Xiaorui Zhang:** Validation, Data curation. **Liang Shan:** Supervision, Project administration. **Chen Jun:** Resources, Funding acquisition.

Declaration of competing interest

Zhenxing Song reports financial support was provided by Hunan Kejing New Energy Technology Co., Ltd. If there are other authors, they declare that they have no known competing financial interests or personal relationships that could have appeared to influence the work reported in this paper.

References

[1] Z. Wang, L. Wu, J. Zhou, B. Shen, Z. Jiang, Enhanced microwave absorption of Fe_3O_4 nanocrystals after heterogeneously growing with ZnO nanoshell, RSC Adv. 3 (2013) 3309, https://doi.org/10.1039/c2ra23404a.

[2] Y. Liu, J. Qin, L. Lu, J. Xu, X. Su, Enhanced microwave absorption property of silver decorated biomass ordered porous carbon composite materials with frequency selective surface incorporation, Int. J. Miner. Metall. Mater. 30 (2023) 525–535, https://doi.org/10.1007/s12613-022-2491-7.

[3] B. Lu, X.L. Dong, H. Huang, X.F. Zhang, X.G. Zhu, J.P. Lei, J.P. Sun, Microwave absorption properties of the core/shell-type iron and nickel nanoparticles, J. Magn. Magn Mater. 320 (2008) 1106–1111, https://doi.org/10.1016/j.jmmm.2007.10.030.

[4] M.S. Seyed Dorraji, M.H. Rasoulifard, A.R. Amani-Ghadim, M.H. Khodabandeloo, M. Felekari, M.R. Khoshrou, I. hajimiri, Microwave absorption properties of polypyrrole-$SrFe_{12}O_{19}$-TiO_2-epoxy resin nanocomposites: optimization using response surface methodology, Appl. Surf. Sci. 383 (2016) 9–18, https://doi.org/10.1016/j.apsusc.2016.04.108.

[5] S.J. Yan, L. Zhen, C.Y. Xu, J.T. Jiang, W.Z. Shao, Microwave absorption properties of $FeNi_3$ submicrometre spheres and SiO_2@$FeNi_3$ core–shell structures, J. Phys. Appl. Phys. 43 (2010) 245003, https://doi.org/10.1088/0022-3727/43/24/245003.

[6] N. Sudrajat, Y. Taryana, D. Dedi, W.A. Adi, L. Darmawan, A. Manaf, Hard magnetic and broadband microwave absorption characteristics of heat-treated Pr_{15}-$XDyXFe_{77}B_8$(x = 0, 1, 2, and 3) alloys, Heliyon 8 (2022) 1, https://doi.org/10.1016/j.heliyon.2022.e10707.

[7] A. Lu, E.L. Salabas, F. Schüth, Magnetic nanoparticles: synthesis, protection, functionalization, and application, Angew. Chem. Int. Ed. 46 (2007) 1222–1244, https://doi.org/10.1002/anie.200602866.

[8] X. Cao, Z. Jia, D. Hu, et al., Synergistic construction of three-dimensional conductive network and double heterointerface polarization via magnetic FeNi for broadband microwave absorption, Adv. Compos. Hybrid Mater. 5 (2) (2022) 1030–1043. https://link.springer.com/article/10.1007/s42114-021-00415-w.

[9] M. Feygenson, A. Kou, L.E. Kreno, A.L. Tiano, J.M. Patete, F. Zhang, M.S. Kim, V. Solovyov, S.S. Wong, M.C. Aronson, Properties of highly crystalline NiO and Ni nanoparticles prepared by high-temperature oxidation and reduction, Phys. Rev. B 81 (2010) 014420, https://doi.org/10.1103/PhysRevB.81.014420.

[10] L. Sun, Z. Jia, S. Xu, M. Ling, D. Hu, X. Liu, C. Zhang, G. Wu, Synthesis of $NiCo_2$-0.5xCr_2O_3@C nanoparticles based on hydroxide with the heterogeneous interface for excellent electromagnetic wave absorption properties, Compos. Commun. 29 (2022) 100993, https://doi.org/10.1016/j.coco.2021.100993.

[11] L. Wang, H. Guan, S. Su, J. Hu, Y. Wang, Magnetic FeO_X/biomass carbon composites with broadband microwave absorption properties, J. Alloys Compd. 903 (2022) 163894, https://doi.org/10.1016/j.jallcom.2022.163894.

[12] H. Soleimani, J.Y. Yusuf, L.K. Chuan, H. Soleimani, M.L. Bin Sabar, A. Öchsner, Z. Abbas, A.I. Balogun, G. Kozlowski, In-situ preparation of $CoFe_2O_4$ nanoparticles on eggshell membrane-activated carbon for microwave absorption, Heliyon 9 (2023) e13256, https://doi.org/10.1016/j.heliyon.2023.e13256.

[13] P. Toneguzzo, G. Viau, O. Acher, F. Fiévet-Vincent, F. Fiévet, Monodisperse ferromagnetic particles for microwave applications, Adv. Mater. 10 (1998) 1032–1035, https://doi.org/10.1002/(SICI)1521-4095(199809)10:13<1032.

[14] A. Das, P. Negi, S.K. Joshi, A. Kumar, Enhanced microwave absorption properties of Co and Ni co-doped iron (II,III)/reduced graphene oxide composites at X-band frequency, J. Mater. Sci. Mater. Electron. 30 (2019) 19325–19334, https://doi.org/10.1007/s10854-019-02293-x.

[15] Y. Bi, M. Ma, Z. Liao, Z. Tong, Y. Chen, R. Wang, Y. Ma, G. Wu, One-dimensional Ni@Co/C@PPy composites for superior electromagnetic wave absorption, J. Colloid Interface Sci. 605 (2022) 483–492, https://doi.org/10.1016/j.jcis.2021.07.050.

[16] J. Liu, M.-S. Cao, Q. Luo, H.-L. Shi, W.-Z. Wang, J. Yuan, Electromagnetic property and tunable microwave absorption of 3D nets from nickel chains at elevated temperature, ACS Appl. Mater. Interfaces 8 (2016) 22615–22622, https://doi.org/10.1021/acsami.6b05480.

[17] H. Guo, B. Pu, H. Chen, J. Yang, Y. Zhou, J. Yang, B. Bismark, H. Li, X. Niu, Surfactant-assisted solvothermal synthesis of pure nickel submicron spheres with microwave-absorbing properties, Nanoscale Res. Lett. 11 (2016) 352, https://doi.org/10.1186/s11671-016-1562-y.

[18] J. Wang, X. Jia, T. Wang, S. Geng, C. Zhou, F. Yang, X. Tian, L. Zhang, H. Yang, Y. Li, Synthesis and microwave absorption property of two-dimensional porous nickel oxide nanoflakes/carbon nanotubes nanocomposites with a threaded structure, J. Alloys Compd. 689 (2016) 366–373, https://doi.org/10.1016/j.jallcom.2016.07.328.

[19] S.-S. Yu, C.-L. Chang, C.R.C. Lee, Wang, Gold nanorods: electrochemical synthesis and optical properties, J. Phys. Chem. B 101 (1997) 6661–6664, https://doi.org/10.1021/jp971656q.

[20] B.-X. Chung, C.-P. Liu, Synthesis of cobalt nanoparticles by DC magnetron sputtering and the effects of electron bombardment, Mater. Lett. 58 (2004) 1437–1440, https://doi.org/10.1016/j.matlet.2003.06.018.

[21] H. Wang, H.Y. Jeong, M. Imura, L. Wang, L. Radhakrishnan, N. Fujita, T. Castle, O. Terasaki, Y. Yamauchi, Shape- and size-controlled synthesis in hard templates: sophisticated chemical reduction for mesoporous monocrystalline platinum nanoparticles, J. Am. Chem. Soc. 133 (2011) 14526–14529, https://doi.org/10.1021/ja2058617.

[22] H. Masuda, K. Fukuda, Ordered metal nanohole arrays made by a two-step replication of honeycomb structures of anodic alumina, Science 268 (1995) 1466–1468, https://doi.org/10.1126/science.268.5216.1466.

[23] P. Baghel, A.K. Sakhiya, P. Kaushal, Ultrafast growth of carbon nanotubes using microwave irradiation: characterization and its potential applications, Heliyon 8 (2022) e10943, https://doi.org/10.1016/j.heliyon.2022.e10943.

[24] F. Wen, F. Zhang, Z. Liu, Investigation on microwave absorption properties for multiwalled carbon nanotubes/Fe/Co/Ni nanopowders as lightweight absorbers, J. Phys. Chem. C 115 (2011) 14025–14030, https://doi.org/10.1021/jp202078p.

[25] E. Mosquera-Vargas, R. Tamayo, M. Morel, M. Roble, D.E. Díaz-Droguett, Hydrogen storage in purified multi-walled carbon nanotubes: gas hydrogenation cycles effect on the adsorption kinetics and their performance, Heliyon 7 (2021) e08494, https://doi.org/10.1016/j.heliyon.2021.e08494.

[26] G.-M. Shi, S.-H. Lv, X.-B. Cheng, X.-L. Wang, S.-T. Li, Enhanced microwave absorption properties of modified Ni@C nanocapsules with accreted N doped C shell on surface, J. Mater. Sci. Mater. Electron. 29 (2018) 17483–17492, https://doi.org/10.1007/s10854-018-9848-8.

[27] G.P. Abhilash, D. Sharma, S. Bose, C. Shivakumara, PANI-wrapped $BaFe_{12}O_{19}$ and $SrFe_{12}O_{19}$ with rGO composite materials for electromagnetic interference shielding applications, Heliyon 9 (2023) e13648, https://doi.org/10.1016/j.heliyon.2023.e13648.